Electronic phase separation transition as the origin of the superconductivity and pseudogap phase of cuprates

2009 J. Phys.: Condens. Matter 21 235701

(http://iopscience.iop.org/0953-8984/21/23/235701)

IOP PUBLISHING JOURNAL OF PHYSICS: CONDENSED MATTER

J. Phys.: Condens. Matter **21** (2009) 235701 (6pp) doi:10.1088/0953-8984/21/23/235701

Electronic phase separation transition as the origin of the superconductivity and pseudogap phase of cuprates

E V L de Mello, R B Kasal and C A C Passos

Instituto de Física, Universidade Federal Fluminense, Niterói, RJ 24210-340, Brazil

Received 10 March 2009, in final form 14 April 2009
Published 7 May 2009
Online at stacks.iop.org/JPhysCM/21/235701

Abstract

To deal with the physics of cuprate superconductivity we propose an electronic phase separation transition that segregates the holes into high and low density domains. The calculated grain boundary potential favors the development of intragrain superconducting amplitudes. The zero resistivity transition arises only when the intergrain Josephson coupling E_J is of the order of the thermal energy and phase locking takes place among the superconducting grains. We show that this approach explains the pseudogap and superconducting phases and it also reproduces some recent scanning tunneling microscopy data.

(Some figures in this article are in colour only in the electronic version)

1. Introduction

The nature of the pseudogap phase has been widely recognized to be the key to understanding the physics of cuprate superconductors and their complex phase diagram [1, 2]. At present, there is no consensus on its origin and also no agreement on the detailed generic doping dependence p of the pseudogap temperature $T^*(p)$ [2]. This difficulty in finding a unified explanation for the data collected in many different experiments is certainly due to the intricate charge dynamics of cuprate superconductors.

To deal with these complicated charge dynamics we have previously proposed a static phase separation [3–6] based on the experimental evidence of ion diffusion in $La_2CuO_{4+\delta}$ and in Bi2212 above room temperature. The experimental data are consistent with phase separation at the upper pseudogap $T^0(p)$ (in the notation of [1]) and consequently the ionic segregation transition must occur at a higher temperature $T_{PS}(p)$. Since $T^0(p)$ (and $T_{PS}(p)$) falls to zero in the overdoped regime and ionic mobility requires high temperatures, we previously used a bimodal like charge disorder for underdoped compounds and a continuous Gaussian distribution for overdoped ones [5–7]. However, new scanning tunneling microscopy (STM) data have shown an inhomogeneous local gap structure that remains in the far overdoped regime [8–10] which cannot be explained by an ionic phase separation, due to the low values of $T^0(p)$ for p values larger than 0.2. These new STM results on distinct doping regimes have clearly shown local gaps with different amplitudes at temperatures below and above the zero resistivity transition $T_c(p)$ [9, 10] which rule out ionic phase separation as the sole origin of the cuprate inhomogeneities.

Here, in order to have a unified description of the STM data in the overdoped and underdoped regions of the phase diagram, we propose a pure electronic phase separation (EPS). Recent resistivity measurements near the superconducting–insulator transition ($p \approx 0.05$) support the idea that holes doped in the system lead to an electronic phase separation state composed of insulating and superconducting regions coexisting at the same time [11, 12]. Our point is that such a transition is driven by the general minimization principle of the thermodynamic free energy. The proximity of the antiferromagnetic (AF) order for a low doping compound drives the system to form zero doping bubbles where this AF order remains locally in order to maximize the entropy or minimize the free energy of the entire system. In this way the electrons (or holes) generate inhomogeneous regions which increase continuously as the temperature decreases below the transition temperature $T_{PS}(p)$ and freeze at lower temperatures. We will show here that this second order EPS transition may be used to explain the increase in superconducting and pseudogap phases.

As mentioned above, the origin of this novel EPS transition is the proximity to the insulator AF phase, common to all cuprates, and it can be described in terms of the general principle of a competing free energy minimum. As the temperature decreases, the free energy of the homogeneous

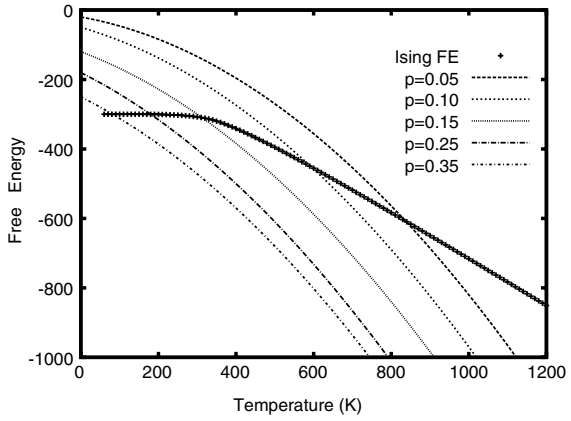

Figure 1. The curves show the difference in free energy $\Delta U_{\rm M}(p) - {\rm FE}_{\rm Mix}(p)$ for some p values. The intersection with AF free energy yields the onset of EPS, i.e. $T_{\rm PS}(p)$. $T_{\rm PS}(p)$ is plotted in figure 2.

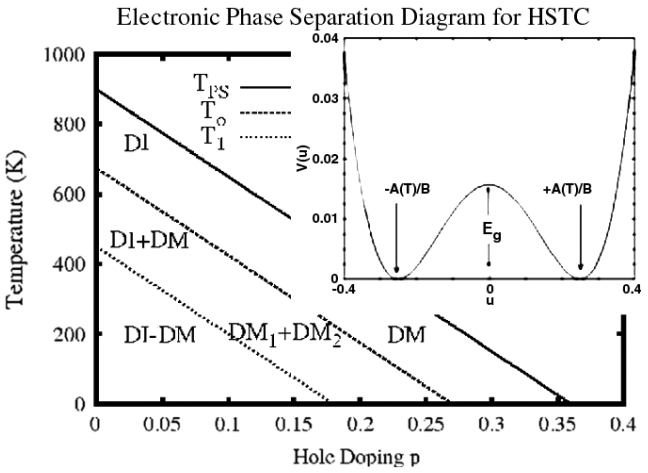

Figure 2. Electronic phase diagram for cuprates. $T_{\rm PS}$ marks the onset of phase separation into the two main densities corresponding to the two minima of the GL potential (equation (3)) as seen in the inset. As the temperature decreases below $T_{\rm PS}(p)$, the potential barrier $E_{\rm g}$ increases and the two minima at $\pm A(T)/B$ separate from each other.

system with average density p becomes lower than the anisotropic one for a granular bimodal distribution [3] of AF domains with $p(i) \approx 0$ and high hole density domains with $p(i) \approx 2p$. This condition can be written as

$$ {\rm FE}^{\rm 2D}{}_{\rm Is} \leqslant -\Delta U_{\rm M} - {\rm FE}_{\rm Mix}(2p). \qquad (1) $$

Here $\Delta U_{\rm M}(p) = 3p^2 U_{\rm M}^{(0)} + \gamma p T^2/2$ is the difference between the free energy of a homogeneous fermion gas with density p and the separate portion with hole density $2p$, which is mixed with $\rm FE_{Is}^{2D}$—the Onsager specific free energy for a 2D Ising model with a spin coupling value that yields a Néel temperature at $T = 350$ K—taken as a model for the AF phase [13]. ${\rm FE}_{\rm Mix}(p)$ is the free energy of mixing [14]. In figure 1 we show the condition for the onset of the EPS transition for some selected values of average density p, when the lines cross the $\rm FE_{Is}^{2D}$. The used value of γ is consistent with the entropy measurements for cuprates [15]. The calculated $T_{\rm PS}(p)$ are in general agreement with the upper pseudogap values $T^0(p)$ [1, 2] and, more importantly, *it provides a physical interpretation for the origin of the electronic inhomogeneities in the cuprates.*

2. The electronic phase separation

Now that we have discussed why cuprates may go through a transition to form granular charge domains, we need a quantitative description of such a transition. For this purpose we use the theory of Cahn–Hilliard (CH) [14] that is appropriate for describing phase separation transitions. The difference between the local and the average charge density $u(i, T) \equiv ((p(i, T) - p)/p)$ is the transition order parameter, and $|u| \leqslant 1$. Clearly $u(i, T) = 0$ corresponds to a homogeneous system above the phase separation onset temperature $T_{\rm PS}(p)$. Then the typical Ginzburg–Landau (GL) free energy functional in terms of such an order parameter near the transition is given by

$$ f(i, T) = \tfrac{1}{2}\varepsilon^2 |\nabla u(i, T)|^2 + V(u(i, T)) \qquad (2) $$

where the potential $V(u, T) = A^2(T)u^2/2 - B^2u^4/4 + \cdots$, $A^2(T) = \alpha(T_{\rm PS}(p) - T)$, and α and B are constants that lead to lines of fixed values of $A(T)/B$, parallel to $T_{\rm PS}(p)$, as shown in figure 2. The parameter ε gives the size of the grain boundaries between two low and high density phases $p_{\pm}(i)$ [4, 16]. The energy barrier between two grains of distinct phases is $E_{\rm g}(T) = A^4(T)/B$, which is proportional to $(T_{\rm PS} - T)^2$ near the transition, and becomes nearly constant for temperatures close to $T_{\rm PS}(p)$. Thus, hereafter we will use $E_{\rm g}(p, T) \equiv V(p, T)$ as the grain boundary potential (see the inset of figure 2). $V(p, T) = V(p) \times V(T)$, and we assume, for simplicity, that $V(p)$ has a linear behavior on p and that its temperature equipotentials are parallel to $T_{\rm PS}(p)$. In figure 2 we plot where the EPS transition should start, i.e. $T_{\rm PS}(p)$, and where it is detected, namely at the upper pseudogap $T^0(p)$ (according to [1]), both approximated by a linear function on p. The others lines shown in the figure, like $T_1(p)$, represent the different degrees of phase separation, which depends on the values of $A(T_{\rm PS} - T)/B$.

For completeness, the CH equation can be written [17] in the form of a continuity equation of the local free energy density f, $\partial_t u = -\nabla \cdot \mathbf{J}$, with the current $\mathbf{J} = M\nabla(\delta f/\delta u)$, where M is the mobility or the charge transport coefficient. Therefore,

$$ \frac{\partial u}{\partial t} = -M\nabla^2(\varepsilon^2\nabla^2 u + A^2(T)u - B^2u^3). \qquad (3) $$

We have already made a detailed study of the evolution of the density profile in a 105×105 array as function of the time steps, up to the stabilization of the local densities, for parameters that yield stripe [5] and patchwork [4, 18] patterns relevant for high critical temperature superconductors (HTSCs).

The temperature evolution of the second order EPS is studied with the ratio $A(T)/B$ [18]. $A(T)/B = 0.2$ is close to the value of the measured upper pseudogap temperature

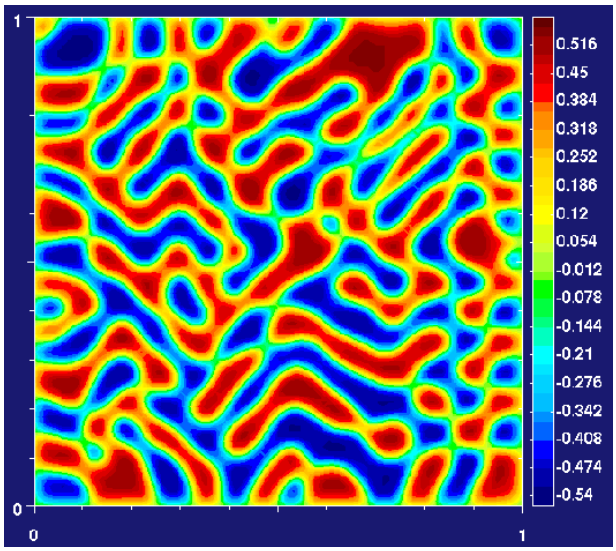

Figure 3. The charge density map on a 105 × 105 system after 6400 time steps. $A(T, p)/B = 0.6$, which corresponds to values of T close to the line T_1 plotted in figure 2, i.e. with $0.05 < p < 0.18$. The dark (blue) grains are in the verge of becoming insulators (low local density) and the light (red) ones are metallic like (large local density).

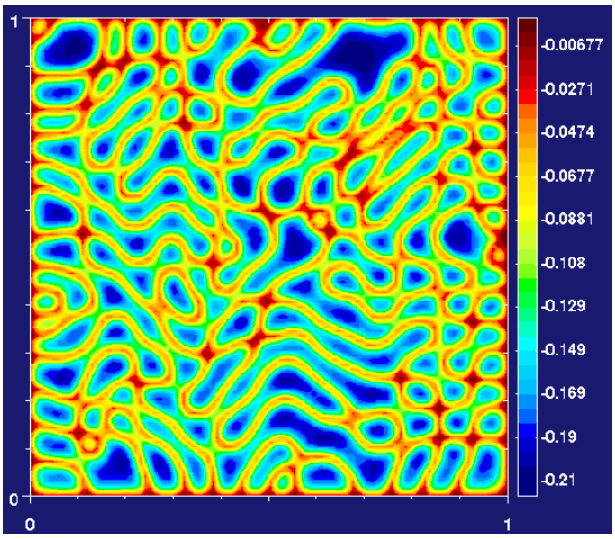

Figure 4. Density profile of the local free energy (in arbitrary units) in the same location and temperature as in figure 3. The lighter (red) lines show the potential barrier among the grain boundaries. In this way the system becomes a mixture of two disordered metals with high and low densities (DM1 + DM2) or a mixture of (local) low density insulators and (local) high density metallic like grains.

$T^0(p)$ shown in figure (2) and it is where the process of phase segregation becomes measurable.

At $A(T)/B = 0.6$ the system is close to the T_1 line, i.e. at a level of disorder at which the low density grains are insulator like and the high density ones are metallic. This crossover line between two disordered metals and a mixture of metal and insulator grains has been seen in many experiments [2]. In this case, the EPS domains are clearly formed, as displayed in figure 3, and the system is on the limit between a disordered metal with grains of two densities and a mixture of metallic and insulator (AF) grains. This is possibly the origin of the instability that falls to zero near $p = 0.18$, as seen in many experiments [2, 15, 19] but not detected by the STM data for the Bi2212 series [8]. At $T \approx 0$ K the domains are frozen, and in general the low density insulator regions decrease in number and size as p increases, but even overdoped samples have some remaining AF grains according to our simulations, as also experimentally verified by neutron diffraction data [20].

In order to estimate the potential that confines the holes into the grains and its connection to the superconducting phase, we study the evolution of free energy with time and temperature together with the corresponding density profile. In figure 4 we show the free energy map associated with the density profile of figure 3, both made by the same computer simulation. It shows that the low and high density grains, at this temperature (60% of T_{PS}), are already bound regions of the free energy minimum.

As the temperature decreases below T_{PS}, using similar simulations to the one shown in figure 4 for various values of temperature, it is clear that the potential barrier among the grains or the intragrain potential $V(p, T)$ increases and becomes constant at low temperatures and low p. Consequently the holes become confined by this effective attraction toward the center of the grains and it may be taken as *the origin of the superconducting interaction* that forms the (intragrain) hole pairs.

3. The superconducting calculations

Intragrain superconductivity is naturally studied with the Bogoliubov–de Gennes (BdG) theory in a similar fashion to we did before for a phenomenological potential and a static phase separation [4–6]. The calculations are performed on a square lattice of 32 × 32 sites, that is, on a small part of the charge density profile given in figure 3.

Taking the extended Hubbard Hamiltonian to describe the hole dynamics, the diagonalizing process is made by the BdG equations [4–6, 18] with the hopping value $t = 0.15$ eV, next neighbor hopping $t_2 = 0.70t$, on-site repulsion $U = 1.3t$ and, most importantly, the EPS next neighbor attraction $V(p, T) \equiv E_g(p, T)$ derived from grain boundary values or grain confining potential. Except for the temperature dependent $V(p, T)$ all the others parameters are similar to values previously used [4–6], although in a different context, since here we are dealing with electronic phase separation.

Following our free energy simulations, from low temperatures up to $T_{PS}(p)$ when the grains melt down, we can obtain the qualitative behavior of the grain boundary potential $E_g(p, T)$. In order to yield average coherent gap values comparable with the STM data on $0.11 \leqslant p \leqslant 0.19$ Bi2212 compounds [8], we find a set of parameters that can be written as

$$E_g(p, T) = V(p) \times V(T) = (-0.9 + 2.8 \times p) \times (1 - T/T_{PS})^{(3-T/T_{PS})}, \quad (4)$$

where the values are in eV, $V(p)$ is linear and vanishes at $p \approx 0.32$ following a linear approximation to $T_{PS}(p)$. $V(T)$ falls to zero near $T_{PS}(p)$ and increases towards $T = 0$ K.

In general, the CH and BdG combined calculations yield very low or almost zero local gaps for the regions with low densities, i.e. $p(i) \leqslant 0.09$. For grains with larger local densities $p(i) \geqslant 0.1$, the local Fermi level is large enough to have d-wave superconducting amplitudes $\Delta_d(i, T)$. We define the *local superconducting temperature* $T_c(i)$ as the temperature at which $\Delta_d(i, T)$ arises in one given site 'i'. *The largest value of* $T_c(i)$ *in a given compound determines the pseudogap temperature* $T^*(p)$ which marks the onset of superconductivity. Since $T^*(p)$ is closely related to the potential $V(p, T)$ it also increases in the overdoped region [21], similar to the Nernst effect [22] in many other experiments [1, 2].

As the temperature decreases below $T^*(p)$ and some high density grains become superconductors, the zero resistivity transition takes place when the Josephson coupling E_J among these grains is sufficiently large to overcome thermal fluctuations, i.e. $E_J(p, T = T_c) \approx k_B T_c(p)$, which leads to phase locking and long range phase coherence. Consequently the superconducting transition in cuprates occurs in two steps, similar to a superconducting material embedded in a non-superconducting matrix [23], first by the appearance of intragrain superconductivity and then by Josephson coupling with phase locking at a lower temperature, *which provides a clear interpretation for the pseudogap phase*. Since $T_c(p)$ is not directly related to the local or intragrain superconductivity, the gaps $\Delta_d(i, T)$ do not change appreciably around $T_c(p)$, especially for underdoped compounds that have large $T^*(p)$. This fact is verified experimentally by temperature dependent tunneling [24] and angle resolved photon emission [25] experiments.

4. Results and discussions

Using the theory of granular superconductors [26], $E_J(p, T) \propto C_N(p) \times \Delta(p, T)$ where $C_N(p)$ is the normal conductivity among the grains. As shown in figure (3), the grain boundaries are made of walls with the mean density p surrounding the grains. On the other hand, the conductivity increases by a few orders of magnitude with p in the Cu–O plane [27] and $C_N(p)$ is small in the underdoped region. That is just the opposite of the average behavior of $\Delta_d(i, T)$, which, following $V(p, T)$, decreases as p increases. This gives some insight into the superconducting 'dome shape' of the resistivity transition with the maximum T_c around $p = 0.16$ in the middle of the EPS region ($T_{PS}(p \approx 0.32) = 0$). Also $E_J \propto J_c r_i^2$, where J_c is the critical current density and r_i is the average size of the grains. Taking typical optimum doping values [28], i.e. $J_c \approx 10^7$ A m^{-2} and $r_i \approx 50$ Å, as one can see directly from our figure (3) we get $E_J \approx 8$ meV or $T_c \approx 90$ K, which is a good estimate for the Bi2212 optimum T_c.

Now we turn to the new STM data that motivated the introduction of the EPS concept instead of ionic phase separation as the origin of the HTSC inhomogeneities, which was the idea we first developed in earlier papers [4]. We first notice the presence of the $p \approx 0$ AF insulator ($p(i) \leqslant 0.03$) and even low density domains ($p(i) \leqslant 0.09$) which are closer to the half filled band and require a high energy cost to accept extra electrons; this explains why injection of electrons produces less STM current than extraction and also why this asymmetry increases drastically as p decreases [29].

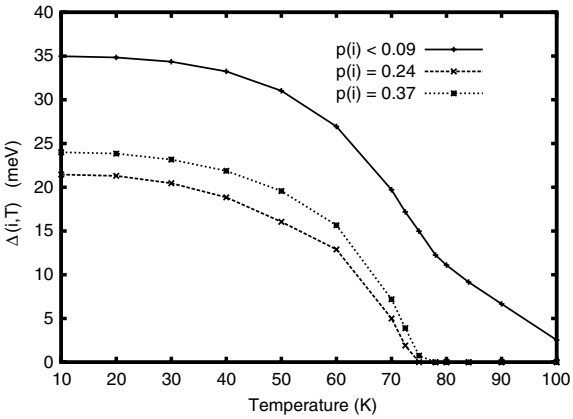

Figure 5. The BdG calculation for $\Delta_d(i, T)$ at three locations on the 32×32 mesh with average hole doping $p \sim 0.24$. For local $p(i) \leqslant 0.9$ the grains are insulator like, and the associated gaps are not superconducting. Instead the STM signals are from activation over the grain boundary potential and from the neighboring superconducting grains with $\Delta_d(j, T)$.

Figure 5 shows some of the local BdG superconducting amplitude calculations at selected points in the Cu–O plane, as in figure 3, for comparison with the high temperature STM data of overdoped ($p \approx 0.22$–0.24) Bi2212 compounds [9, 10]. The smaller coherent gaps $\Delta_d(i, T)$ are calculated for two random different locations in metallic grains. The larger gaps originated in the insulator grains and they are due to activation over the grain boundary barrier $B_{ij}(T)$ that is derived from the grain boundary potential $V(p, T)$ and the calculated $\Delta_d(j, T)$ from a neighboring metallic grain j. As one can see in the local gap maps from the STM experiments, at temperatures above $T_c(p)$ they are always surrounded by a small superconducting region [9, 10]. Another result of the BdG local superconducting calculations is that, despite the uncertainty on $T_c(i)$ for very small gaps, the results like those displayed in figure 3 follow closely the experimentally measured relation $2\Delta_d(i, T = 0\ \text{K})/k_B T_c(i) \approx 8$ [9].

The local superconducting gap can be also obtained in the context of the BdG equations through the study of the local density of states (LDOS), which is given by

$$N_i(E) = \sum_n [|u_n(\mathbf{x}_i)|^2 f_n'(E - E_n) + |v_n(\mathbf{x}_i)|^2 f_n'(E + E_n)], \tag{5}$$

where the prime is the derivative with respect to the argument. This equation allows us to calculate the local gap at any point 'i' or any location of an inhomogeneous system at any temperature. E_n are the eigenvalues of the BdG equation. The difference between this equation and the calculations of $\Delta_d(i, T)$ is that it yields any suppression in the LDOS, whether from superconducting or for any other process, like bound

states in the low density grains. Following the CH calculations, we study the LDOS on a sample as shown in figure 3.

In panel (a) of figure 6 we show the ratio LDOS(T)/LDOS (60 K) for an overdoped compound with $p \approx 0.235$ at a high density puddle (with $p(i_0) \approx 2p$) where the d-wave superconducting amplitude is $\Delta_d(i_0, t = 0) = 0.24$ meV, one of the largest in the system. This choice of p is only for comparison with the STM experimental results [10]. As in figure 5 the local amplitude goes to zero near $T_c(i_0) \approx 72$ K. In panel (b) we study the LDOS in a low density cluster at a point with $p(i)$ almost zero, i.e. at a location inside an AF grain. In this case, the local amplitude $\Delta(i, T) = 0$ and the large peaks seen in the figure are local pseudogaps which are related to the inhomogeneous potential of the phase separation. They are generally 50–70% larger than a typical superconducting (coherent) gap in the sample with $p \approx 0.23$. This shows unequivocally the presence of a pseudogap as it comes from the phase separation or grain boundary electronic confining potential that suppress spectral weight, and it is present everywhere. The origin of the pseudogap is clearly due to the inhomogeneities in the local charge density because it is completely absent in calculation with homogeneous densities. Notice that the pseudogap is almost constant at low temperatures but decreases as the temperature increases because overdoped samples have a low phase separation temperature T_{PS}. In panel (c) of figure 6, as a demonstration that the pseudogap is present everywhere, we calculate the LDOS also at the same location as for the calculations in panel (a) but at a large bias interval to enclose both the superconducting gap and the pseudogap.

Notice that the result displayed in figure 6(c) resembles the results from tunneling spectroscopic measurements [30], especially those where the superconducting gap and the pseudogap are distinguished [31]. As was clear in these studies, the superconducting gap is much more sensitive to the temperature than the pseudogap. However, we can see in figures 6(b) and (c) that pseudogap also varies with the temperature, but this effect is stronger in the overdoped regime, as in the compound we are dealing with ($p = 0.23$), due to the low values of $T_{PS}(p)$. For underdoped compounds the pseudogap changes very little with temperature near to and below the critical temperature $T_c(p)$, and this will be subject of another publication.

One of the main consequences of our calculations is shown in figures 6(a) and (b). The STM measurements by Pasupathy *et al* [10] demonstrated that the local conductivity (dI/dV, where I is local current and V the applied bias) is lower in regions with larger gaps. This result is completely unexpected, because the gaps measured by STM were believed to be all d-wave superconducting ones and, consequently, larger local gaps are associated with larger local densities and greater local metallic behavior. Figure 6(b) shows a large pseudogap in a low density region where the BdG calculations yield zero superconducting amplitude which always occurs at the grains with very low local hole density. Usually the pseudogaps are larger than the superconducting gaps, and as we have shown they occur in the very low density grains which display a more insulator-like behavior, in agreement with the findings of Pasupathy *et al* [10] (see their figures 4(a)–(c)).

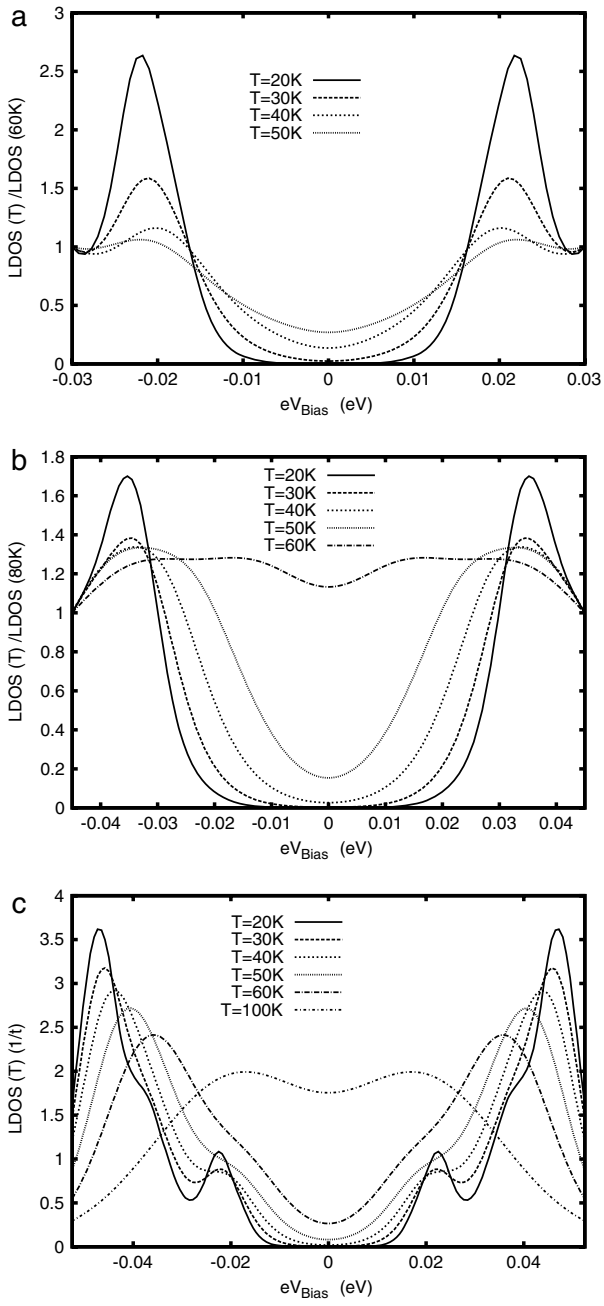

Figure 6. (a) The calculated LDOS at a location with one of the largest local superconducting d-wave gaps, namely $\Delta_d \approx 20$ meV. (b) The LDOS at a location without d-wave superconducting amplitude; nevertheless the LDOS displays a suppression in the spectral weight associated with the pseudogap. (c) Calculations for the same place as in panel (a) but at a larger bias interval in order to capture both the pseudogap and the d-wave gap.

5. Conclusions

In conclusion we have proposed a new universal electronic phase in cuprate superconductors driven by the general thermodynamics principle of minimum free energy. The presence of AF order in the parental compound generates competition between an electronic homogeneous system and one composed of low density grains and grains with local

AF order and high density. Consequently, as the temperature decreases below the transition temperature the system becomes essentially made of disordered low and high charge density grains or puddles and their local doping differences are larger at lower temperatures. The grains are essentially static but melt slowly and disappear near $T_{PS}(p)$, generating the complex behavior of the normal HTSC phase. The different lower pseudogap lines detected in many experiments, some falling to zero temperature near $p = 0.19$ and some near the superconductivity onset at $p = 0.27$, are likely to be different aspects of the varying disorder of this second order phase transition. The grain boundary potential confines the holes to nanoscopic regions and gives rise to the superconducting pairing potential.

Such an anomalous phase arises due to the proximity to the AF undoped insulator, and may be common to other materials with similar doping dependent phases, like manganites which also possess a pseudogap phase [32]. The understanding of these features may open the possibility of new technologies and the development of materials with a large resistivity transition T_c.

Acknowledgment

We gratefully acknowledge partial financial aid from Brazilian agency CNPq.

References

[1] Timusk T and Statt B 1999 *Rep. Prog. Phys.* **62** 61
[2] Tallon J L and Loram J W 2001 *Physica* C **349** 53
[3] de Mello E V L *et al* 2003 *Phys. Rev.* B **67** 024502
[4] de Mello E V L and Caixeiro E S 2004 *Phys. Rev.* B **70** 224517
[5] de Mello E V L and Dias D N 2007 *J. Phys.: Condens. Matter* **19** 086218
[6] Dias D N *et al* 2008 *Physica* C **468** 480
[7] Dias D N *et al* 2007 *Phys. Rev.* B **76** 90737
[8] McElroy K *et al* 2005 *Phys. Rev. Lett.* **94** 197005
[9] Gomes Kenjiro K *et al* 2007 *Nature* **447** 569
[10] Pasupathy Abhay N *et al* 2008 *Science* **320** 196
[11] Oh S, Crane T A, Van Harlingen D J and Eckstein J N 2006 *Phys. Rev. Lett.* **96** 107003
[12] Salluzzo M *et al* 2008 *Phys. Rev.* B **78** 054524
[13] Stanley H E (ed) 1971 *Introductin to Phase Transitions and Critical Phenomena* (New York: Oxford University Press) p 122
[14] Cahn J W and Hilliard J E 1958 *J. Chem. Phys.* **28** 258
[15] Loram J W *et al* 2001 *J. Phys. Chem. Solids* **62** 59
[16] de Mello E V L and Silveira Filho O T 2005 *Physica* A **347** 429
[17] Bray A J 1994 *Adv. Phys.* **43** 347
[18] de Mello E V L *et al* 2009 *Proc. SCES08*; *Physica* B at press
[19] Sonier J E *et al* 2008 *Phys. Rev. Lett.* **101** 117001
[20] Wakimoto S *et al* 2003 *Phys. Rev. Lett.* **98** 247003
[21] Kruchinin S P 2000 *Physica* C **341–348** 901
[22] Wang Y, Li L and Ong N P 2006 *Phys. Rev.* B **73** 024510
[23] Merchant L *et al* 2001 *Phys. Rev.* B **63** 134508
[24] Suzuki M and Watanbe T 2000 *Phys. Rev. Lett.* **85** 4787
[25] Kanigel A *et al* 2008 *Phys. Rev. Lett.* **101** 137002
[26] Ambeogakar V and Baratoff A 1963 *Phys. Rev. Lett.* **10** 486
[27] Takagi H *et al* 1992 *Phys. Rev. Lett.* **69** 2975
[28] Tallon J L *et al* 1999 *Phys. Status Solidi* **215** 531
[29] Kohsaka Y *et al* 2007 *Science* **315** 1380
[30] Mourachkine A 2005 *Mod. Phys. Lett.* B **19** 743
[31] Krasnov V M, Kovalev A E, Yurgens A and Winker D 2001 *Phys. Rev. Lett.* **86** 2657
[32] Dagotto E *et al* 2003 *Solid State Commun.* **126** 9